# Androgen Receptor Null Male Mice Develop Late-Onset Obesity Caused by Decreased Energy Expenditure and Lipolytic Activity but Show Normal Insulin Sensitivity With High Adiponectin Secretion

**WuQiang Fan,[1] Toshihiko Yanase,[1] Masatoshi Nomura,[1] Taijiro Okabe,[1] Kiminobu Goto,[1] Takashi Sato,[2] Hirotaka Kawano,[2] Shigeaki Kato,[2] and Hajime Nawata[1]**

**Androgen receptor (AR) null male mice ($AR^{L-/Y}$) revealed late-onset obesity, which was confirmed by computed tomography–based body composition analysis. $AR^{L-/Y}$ mice were euphagic compared with the wild-type male ($AR^{X/Y}$) controls, but they were also less dynamic and consumed less oxygen. Transcript profiling indicated that $AR^{L-/Y}$ mice had lower transcripts for the thermogenetic uncoupling protein 1, which was subsequently found to be ligand-dependently activated by AR. We also found enhanced secretion of adiponectin, which is insulin sensitizing, from adipose tissue and a relatively lower expression of peroxisome proliferator–activated receptor-γ in white adipose tissue in comparison to $AR^{X/Y}$ mice. Both factors might explain why the overall insulin sensitivity of $AR^{L-/Y}$ mice remained intact, despite their apparent obesity. The results revealed that AR plays important roles in male metabolism by affecting the energy balance, and it is negative to both adiposity and insulin sensitivity.**
***Diabetes*** **54:1000–1008, 2005**

The etiology of obesity is extremely heterogeneous, in that it is the final result of interactions among genetic, environmental, and psychosocial factors. The androgen receptor (AR) gene may be one of these genetic factors. AR gene repeat variation was shown to be strongly associated with central obesity indexes in older adults (1). Testosterone is an important factor for determining body composition in males. Abdominal obesity is inversely correlated with serum testosterone levels in men but not in women (2). Steady increases in body fat mass accompany the age-dependent decrease in serum testosterone levels in men (3,4), leading to greater morbidity (5). Pathologically hypogonadal men also have a significantly higher fat mass (3,6), which is reversed by testosterone administration (7,8), whereas suppression of serum testosterone in healthy young men increased the percent fat mass and decreased lipid oxidation rates and resting energy expenditure (9).

We generated an AR null (ARKO) mouse line, using a Cre-loxP system (10–12), and found that male ARKO mice ($AR^{L-/Y}$) developed late-onset obesity, whereas neither heterozygous nor homozygous female ARKO mice were affected (10), suggesting a male-specific AR effect on adiposity.

Herein we report the underlying mechanism of late-onset obesity in $AR^{L-/Y}$ mice. Despite a lack of hyperphagia, $AR^{L-/Y}$ mice had lower spontaneous activity and a decreased overall oxygen consumption ratio. We also observed a concomitant decrease in expression of the thermogenic uncoupling protein 1 (UCP-1). In addition, a unique lack of insulin resistance in $AR^{L-/Y}$ mice, despite the obese phenotype, suggests it was related to an enhanced secretion of adiponectin from adipose tissue.

## RESEARCH DESIGN AND METHODS

An ARKO mutant mouse line was established and maintained as described previously (10–12). Heterozygous females were bred to wild-type males (C57BL/6NCrj; Charles River Japan, Tokyo, Japan) to produce ARKO male mice ($AR^{L-/Y}$) and heterozygous females. Their diet (CLEA rodent diet CE-2; Kyudo, Tosu, Saga, Japan) had the following composition: 54.4% carbohydrate, 24.4% protein, 4.4% fat, and 342.2 kcal/100 g. Mice were weighed weekly, and food consumption was measured by weighing the remaining food every 3 days. All animal protocols were approved by the animal care and use committee of Kyushu University.

**Body fat composition analysis.** For computed tomography (CT) analysis of body fat composition, mice were anesthetized with intraperitoneal injections of pentobarbital sodium (Nembutal; Dainippon Pharmaceutical, Osaka, Japan) and then scanned using a LaTheta (LCT-100M) experimental animal CT system (Aloka, Tokyo, Japan). Contiguous 2-mm slice images between L2 and L4 were used for quantitative assessment using LaTheta software (version 1.00). Visceral fat, subcutaneous fat, and muscle were distinguished and evaluated quantitatively.

**Spontaneous activity.** Spontaneous physical activity was measured using a Letica infrared system (Panlab, Barcelona, Spain). The mice were placed in a $45 \times 45$ cm$^2$ infrared frame in which $16 \times 16$ intercepting infrared light beams formed a double grid of infrared cells. The position of the mice within the infrared frame was traced in a real-time manner. An additional upper infrared frame was applied to detect rearing (mouse standing up on its hind legs). Parameters such as distance traveled, speed, rearing number, and duration were analyzed using the Acti-Track program. By setting two speed thresholds

From the [1]Department of Medicine and Bioregulatory Science, Graduate School of Medical Science, Kyushu University, Fukuoka, Japan; and the [2]Institute of Molecular and Cellular Biosciences, Graduate School of Agricultural and Life Sciences, University of Tokyo, Tokyo, Japan.

Address correspondence and reprint requests to Toshihiko Yanase, MD, PhD, Department of Medicine and Bioregulatory Science, Graduate School of Medical Science, Kyushu University, Maidashi 3-1-1, Higashi-ku, Fukuoka, 812-8582 Japan. E-mail: yanase@intmed3.med.kyushu-u.ac.jp.

Received for publication 2 September 2004 and accepted in revised form 6 January 2005.

AR, androgen receptor; BAT, brown adipose tissue; CT, computed tomography; PPAR-γ, peroxisome proliferator–activated receptor-γ; UCP, uncoupling protein; WAT, white adipose tissue.

TABLE 1
List of primers

| Target | Forward | Reverse | Size |
|---|---|---|---|
| UCP-2 | AACAGTTCTACACCAAGGGC | AGCATGGTAAGGGCACAGTG | 471 |
| β-Actin | GCAATGCCTGGGTACATGGTGG | GTCGTACCACAGGCATTGTGATGG | 492 |
| Acetyl CoA carboxylase | GGGACTTCATGAATTTGCTGATTCTCAGTT | GTCATTACCATCTTCATTACCTCAATCTC | 728 |
| Fatty acid synthase | CACAGATGATGACAGGAGATGG | TCGGAGTGAGGCTGGGTTGAT | 205 |
| PPAR-γ coactivator 1 | CGCAGCCCTATTCATTGTTC | TCATCCCTCTTGAGCCTTTC | 364 |
| Sterol regulatory element–binding protein 1c | ATCGGCGCGGAAGCTGTCGGGGTAG | ACTGTCTTGGTTGTTGATGAGCTGGAGCA | 116 |
| Leptin | TCCAGAAAGTCCAGGATGACAC | CACATTTTGGGAAGGCAGG | 212 |
| Carnitine palmitoyl transferase 1 | ATTCTGTGCGGCCCTTATTGGAT | TTTGCCTGGGATGCGTGTAGTGT | 395 |
| Long-chain acyl-CoA dehydrogenase | GCTGCCCTCCTCCCGATGTT | ATGTTTCTCTGCGATGTTGATG | 258 |
| UCP-1 | CACCTTCCCGCTGGACAC | CCCTAGGACACCTTTATACCTAATG | 91 |
| Hormone-sensitive lipase | CCTACTGCTGGGCTGTCAA | CCATCTGGCACCCTCACT | 142 |
| PPAR-γ | TTGACAGGAAAGACAACGGA | GAGCAGAGTCACTTGGTCATT | 246 |
| GLUT4 | TCTCCAACTGGACCTGTAAC | TCTGTACTGGGTTTCACCTC | 221 |
| Muscle-type phosphofructokinase | AGATGGGTGCTAAGGCTATG | TTTTGAGGATTGGCCTCAGC | 218 |
| Muscle-type pyruvate kinase | CATTGCCGTGACTCGAAATC | CATGGTGTTGGTGAATCCAG | 225 |
| Hexokinase I | CGTGGTGCAAAAGATCCGAG | CTGCTCTTAGGCGTTCGTAG | 243 |
| Hexokinase II | TCTCAGATCGAGAGTGACTG | CGTCTCATGCATGACTTTGG | 272 |
| AR | CAGCATTATTCCAGTGGATGG | GGGCACTTGCACAGAGATG | 274 |
| UCP-1 promoter | TCCATTGGCCTCAAACCCTATGAG | AGGCGTGAGTGCAAGAACAAAAGG | 3,850 |

of 2.00 and 5.00 cm/s, the movements were subclassified into resting (slower than 2.00 cm/s), moving slowly (between 2.00 and 5.00 cm/s), and moving fast (faster than 5.00 cm/s). The mice were placed into the frame 5 h before commencing recording to allow familiarization with the surroundings. Recording was started 2 h after the lights were switched off and lasted for 8 h; mice were assessed individually.

**Oxygen consumption measurements.** Mice were fed regular chow, maintained at a constant room temperature (21–23°C), and subjected to oxygen consumption measurements at ~22 weeks of age using a computer-controlled open-circuit indirect calorimeter (Oxymax; Columbus Instruments, Columbus OH). Mice were housed individually in metabolic chambers ($10 \times 20$ cm$^2$) and had free access to food and water. After a 1-h adaptation to the chamber, $V_{O_2}$ was assessed at 4-min intervals for 24 h. All sample data were analyzed using Oxymax Windows software (version 1.0).

**Glucose tolerance and insulin challenge tests.** For the intraperitoneal glucose tolerance test, mice were fasted overnight and then injected with 2 g D-glucose/kg body wt i.p. Tail blood glucose levels were monitored before and at 15, 30, 60, 90, and 120 min after injection using blood glucose meters (Matsushita Kotobuki Electronics Industries, Ehime, Japan). For the insulin challenge test, mice were fasted overnight and then injected with 0.7 units regular insulin/kg body wt i.p. Tail blood glucose levels were measured at the same time points as above.

**Histology.** Mice were killed at 45 weeks old after an overnight fast, and blood was collected by cardiac puncture. Subcutaneous white adipose tissue (WAT), interscapular brown adipose tissue (BAT), liver, and kidneys were removed and immersion-fixed in 4% paraformaldehyde. After dehydration, tissue samples were paraffin-embedded in a random orientation, sliced into 10-μm sections, and stained with hematoxylin and eosin.

**Blood chemicals.** Blood was collected at the time of death, and the isolated serum was aliquoted and stored at −20°C until use. All blood chemistry items were measured by SRL (Tokyo, Japan). Plasma full-length adiponectin levels were measured using an enzyme-linked immunosorbent assay system as previously described (13).

**Real-time PCR.** Total RNA was isolated from 100 mg of intraperitoneal WAT or interscapular BAT using an RNeasy Lipid Tissue Mini Kit (Qiagen, Valencia, CA). To remove any possible DNA contamination, on-column digestion of DNA was performed with an RNase-free DNase set (Qiagen). Then, 3 μg of total RNA was subjected to reverse transcription using SuperScript III reverse transcriptase (Invitrogen, Carlsbad, CA) primed by random primers. cDNA was then subjected to real-time PCR analysis to quantify various transcripts, using a LightCycler (Roche Diagnostics, Mannheim, Germany) according to the manufacturer's instructions, as we previously described (14). The forward/reverse primer sequences for each target transcript are shown in Table 1. β-Actin was amplified simultaneously as an internal control. The real-time PCR data for each transcript were calculated as the ratio of β-actin.

**UCP-1 promoter assay.** A 3.85-kb (−3,860 to −10 from the start codon) region of the mouse UCP-1 promoter was amplified by PCR using specific primers (Table 1) and KOD-Plus DNA polymerase (Toyobo, Osaka, Japan) in a T-gradient thermoblock (Biometra Biomedizinische Analytik, Gottingen, Germany), and it was subsequently cloned into the pGL3-Basic (Promega, Madison, WI) vector to construct a UCP-1–Luc reporter. Direct sequencing was then performed to validate the full-length sequence and orientation. The effect of AR on the UCP-1 promoter was analyzed in NIH-3T3-L1 adipocytes by the dual luciferase assay, as described previously (15). Briefly, $1 \times 10^5$ cells/well were seeded into 12-well plates, and UCP-1–Luc and pCMV-AR, or pCMX (empty vector), together with the internal control pRL-CMV vector were cotransfected into the cells by SuperFect (Qiagen). The cells were incubated in $10^{-8}$ mol/l dihydroxytryptamine or its solvent, ethanol, for 24 h and then lysed and subjected to the relative luciferase assay using a LUMAT LB9507 luminometer (Berthold Technologies, Bad Wildbad, Germany).

**Statistical analysis.** Data were expressed as the means ± SD and evaluated by Student's two-tail *t* test or ANOVA, followed by post hoc comparisons with Fisher's protected least significant difference test.

## RESULTS

We previously reported that up to 10 weeks old, $AR^{L-/Y}$ mice had growth retardation compared with the male wild-type ($AR^{X/Y}$) mice, but over the next couple of weeks, their body weight caught up with and then exceeded that of $AR^{X/Y}$ mice and eventually developed into overt obesity (10). These phenomena were not observed in ARKO female mice. In the present study, we performed objective CT-based body composition analysis for mice at 40 weeks of age. Figure 1*A* shows the CT-estimated weights of the adipose tissue and muscle in the area assayed (L2–L4). Although the muscle amount was unchanged, the visceral and subcutaneous fat and total fat of $AR^{L-/Y}$ mice were significantly heavier than those of $AR^{X/Y}$ mice. Figure 1*B* shows representative CT images at the L3 level of $AR^{X/Y}$ (*left*) and $AR^{L-/Y}$ (*right*) mice. $AR^{L-/Y}$ mice had increased fat in both visceral and subcutaneous areas. Thus, increased adiposity, rather than a linear increase in body growth, accounted for the elevated body weight of $AR^{L-/Y}$ mice.

The body weight of $AR^{L-/Y}$ mice at 45 weeks of age was significantly higher than that of $AR^{X/Y}$ mice (Fig. 2*A*), and, consistent with the CT data, perirenal fat pads of $AR^{L-/Y}$ mice were clearly larger that those of $AR^{X/Y}$ mice (data not shown). Despite elevated body weight, the kidneys of

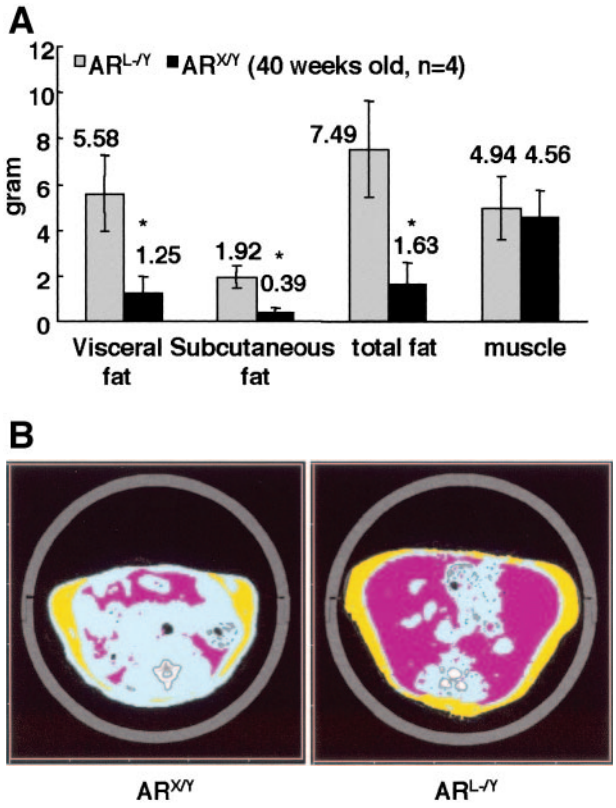


**FIG. 1. CT-based body composition analysis of 40-week-old $AR^{L-/Y}$ and $AR^{X/Y}$ mice. *A*: CT-estimated amounts of visceral fat, subcutaneous fat, and muscle in the abdominal area of L2–L4. *B*: Representative CT images of $AR^{X/Y}$ (*left*) and $AR^{L-/Y}$ (*right*) mice at the L3 level. The pink and yellow areas represent the visceral and subcutaneous fat, respectively. *$P < 0.01$ compared with $AR^{L-/Y}$, $n = 4$.**

$AR^{L-/Y}$ mice were significantly smaller than those of $AR^{X/Y}$ mice (Fig. 2*B*), supporting previous studies demonstrating smaller kidneys in orchidectomized mice (16,17).

In comparison to $AR^{X/Y}$ mice, subcutaneous WAT from $AR^{L-/Y}$ mice was hypertrophic (Figs. 2*C* and *D*). The interscapular BAT in $AR^{L-/Y}$ mice was relatively enlarged and pale (Fig. 2*E*), and it contained higher lipid content (Figs. 2*F* and *G*). A considerable number of cells in $AR^{L-/Y}$ BAT were large and contained unilocular lipid deposits that morphologically mimicked WAT adipocytes (data not shown). Leptin transcript, which is normally restricted to WAT, was elevated in $AR^{L-/Y}$ WAT, as expected (Fig. 2*H*). However, it was also elevated in $AR^{L-/Y}$ BAT (Fig. 2*I*), suggesting that BAT from $AR^{L-/Y}$ mice has characteristics of both BAT and WAT. Thus the BAT of $AR^{L-/Y}$ mice is similar to that from mice in which the genes encoding all three β-adrenergic receptors have been inactivated (18). Despite the apparent obesity, $AR^{L-/Y}$ mice manifested no evidence of fatty liver (data not shown), which is a common consequence of obesity. Because estrogen deficiency has been found to increase WAT in male mice (19,20), and estrogen can be produced by aromatizing testosterone (21), which is severely decreased in $AR^{L-/Y}$ mice because of atrophic testis (12), we addressed the issue of estrogen levels in $AR^{L-/Y}$ mice. We previously reported that at 8 weeks old, before the onset of obesity, serum E2 in $AR^{L-/Y}$ mice was normal (12). In the present study, we found that E2 levels in $AR^{L-/Y}$ mice at 40 weeks of age are still indistinguishable from those in $AR^{X/Y}$ mice (Fig. 2*J*), suggesting $AR^{L-/Y}$ mice are not in short supply of estrogen.

Serum levels of total protein (5.1 ± 0.61 g/dl in $AR^{X/Y}$ mice vs. 4.8 ± 0.9 g/dl in $AR^{L-/Y}$ mice, $n = 6$, $P = 0.49$), blood urea nitrogen (26.5 ± 4.6 mg/dl in $AR^{X/Y}$ vs. 20.8 ± 7.2 g/dl in $AR^{L-/Y}$ mice, $n = 6$, $P = 0.12$), and glucose (78.5 ± 14.2 mg/dl in $AR^{X/Y}$ vs. 88.0 ± 9.9 mg/dl in $AR^{L-/Y}$ mice, $n = 6$, $P = 0.26$) were found unchanged. Those of triglycerides, unesterified free fatty acids, and total cholesterol were also unchanged (10). Serum insulin in $AR^{L-/Y}$ mice tended to be slightly higher, but it did not reach statistical significance (Fig. 3*A*). Unexpectedly, we observed a significant increase in serum adiponectin concentration in $AR^{L-/Y}$ mice (Fig. 3*B*). Adiponectin sensitizes insulin sensitivity via various mechanisms (13,22), and its plasma concentration is negatively correlated with obesity. The unique hyperadiponectinemia in $AR^{L-/Y}$ mice thus prompted us to further evaluate the overall insulin sensitivity. Insulin challenge tests and intraperitoneal glucose tolerance tests were performed on 40-week-old mice. Neither test revealed any differences between the two groups (Figs. 3*C* and *D*), suggesting that overall insulin sensitivity remained intact in $AR^{L-/Y}$ mice, despite their apparent obesity. In contrast to the elevated plasma level of adiponectin, the adiponectin transcript was strikingly decreased in the WAT of obese $AR^{L-/Y}$ mice (Fig. 3*E*), as is commonly observed with obesity. The adiponectin transcript levels were found to be unchanged in $AR^{L-/Y}$ BAT (Fig. 3*F*), ruling out the possibility that BAT, though WAT-like, is an additional adiponectin source. We next carried out CT-based body composition analysis for the whole body to evaluate the relative WAT mass (%WAT) at the whole-body level (%WAT = 100% × whole-body WAT [g]/body weight [g]), and we subsequently estimated the relative total adiponectin production, using the equation: RTAP = %WAT × RAT, where RTAP is the relative total adiponectin production, and RAT is the relative adiponectin transcript copies to β-actin. As shown in Fig. 3*G*, although not statistically different, relative total adiponectin production from $AR^{L-/Y}$ mice was still lower than that from $AR^{X/Y}$ mice. Thus the discordance of adiponectin serum levels and adiponectin transcript levels in WAT still exists because serum adiponectin levels in $AR^{X/Y}$ mice were almost doubled (Fig. 3*B*). Collectively, these data suggest that the intact androgen-AR system of $AR^{X/Y}$ mice is suppressive to the secretion of adiponectin from WAT, whereas $AR^{L-/Y}$ mice had relatively enhanced secretion of the adipokine. In addition to hyperadiponectinemia, we also observed a significant reduction of peroxisome proliferator–activated receptor-γ (PPAR-γ) mRNA in the WAT of $AR^{L-/Y}$ compared with $AR^{X/Y}$ mice (Fig. 3*H*), which might also contribute to the normal insulin sensitivity of $AR^{L-/Y}$ mice (23).

We then studied the molecular events of glucose metabolism in skeletal muscle because muscle is a major target of androgen and adiponectin as well. As shown in Fig. 3*I–M*, although GLUT1 transcript levels were unchanged (data not shown), GLUT4 (muscle-dominant type) levels in $AR^{L-/Y}$ mice were significantly upregulated. The muscle-dominant hexokinase I was also upregulated, although no change was found for hexokinase II. Muscle-type phosphofructokinase tended, albeit not statistically significantly, to

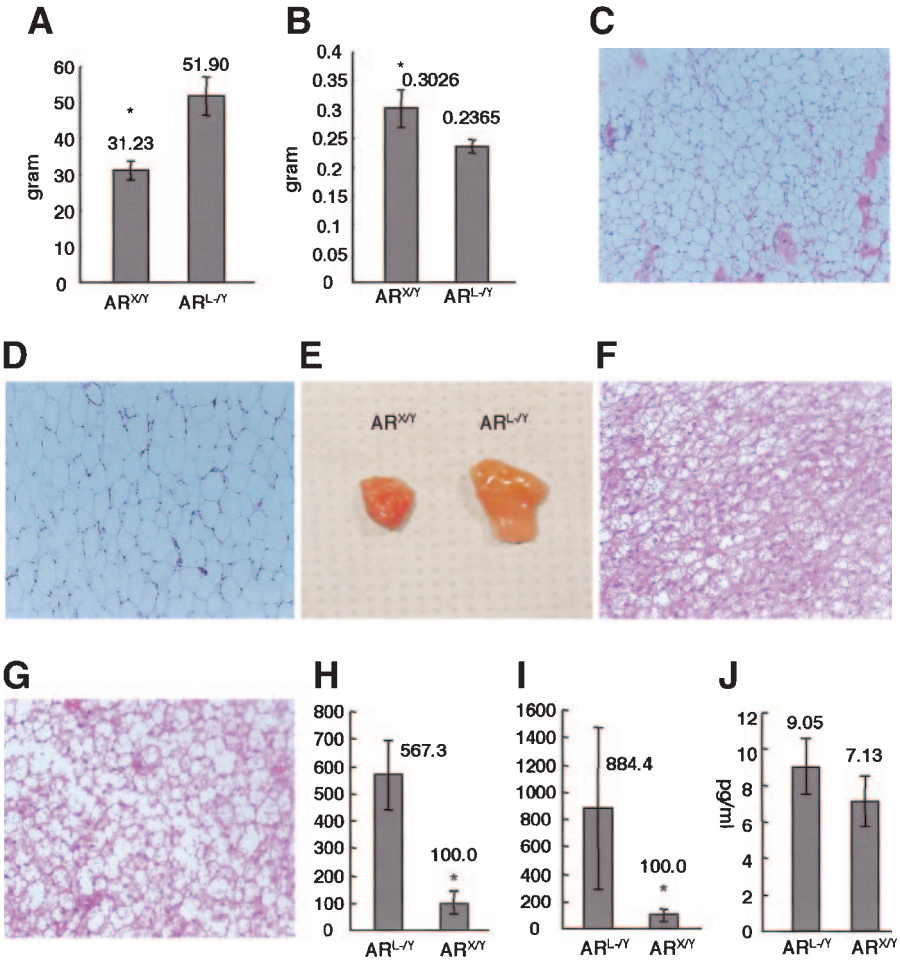


**FIG. 2. General characteristics of late-onset obesity in $AR^{L-/Y}$ mice. *A*: Body weights of 45-week-old $AR^{L-/Y}$ and $AR^{X/Y}$ mice ($n$ = 6). *B*: Kidney weights of 45-week-old $AR^{L-/Y}$ and $AR^{X/Y}$ mice ($n$ = 6). *C* and *D*: The subcutaneous WAT of $AR^{X/Y}$ (*C*) and $AR^{L-/Y}$ mice (*D*), respectively (magnification 100×); it was hypertrophic in $AR^{L-/Y}$ compared with in $AR^{X/Y}$ mice. *E–G*: Interscapular BAT in $AR^{X/Y}$ (*F*) and $AR^{L-/Y}$ mice (*G*); it was enlarged and pale in $AR^{L-/Y}$ compared with in $AR^{X/Y}$ mice (magnification 100× in *F* and *G*). *H* and *I*: Leptin transcript levels in WAT (*H*) and BAT (*I*) in $AR^{X/Y}$ and $AR^{L-/Y}$ mice. The transcript levels in $AR^{X/Y}$ were set at 100. *J*: Serum E2 levels in $AR^{L-/Y}$ and $AR^{X/Y}$ mice. *$P$ < 0.01 compared with $AR^{L-/Y}$ mice, $n$ = 6.**

be higher, whereas increase in muscle-type pyruvate kinase (including muscle-type pyruvate kinase-1 and -2) reached statistical significance. These data suggest glucose uptake and oxidation in muscle might be activated in $AR^{L-/Y}$ mice.

The concept of energy balance, which comprises both energy intake (feeding) and energy expenditure (physical activity, basal metabolism, and adaptive thermogenesis), is the key to understanding obesity (24). We first found that ad libitum food intake was unchanged between $AR^{L-/Y}$ and $AR^{X/Y}$ mice; that is, $AR^{L-/Y}$ mice were euphagic, as already reported (10). Next, we measured spontaneous physical activity for mice at around 8, 20, and 40 weeks of age (Table 2). During the 8-h monitoring period while the lights were off, the 20-week-old $AR^{L-/Y}$ mice ran a significantly shorter distance and showed almost half the number of rearing (standing up on hind legs) behaviors, another important parameter of dynamic behavior, as compared with $AR^{X/Y}$ mice. $AR^{L-/Y}$ mice also showed decreased activity at 40 weeks of age and, importantly, at 8 weeks of age, when the body weight of $AR^{L-/Y}$ mice had not yet exceeded that of $AR^{X/Y}$ mice. This suggests that the reduced activity of $AR^{L-/Y}$ mice is an intrinsic defect but not a secondary effect of the mice being overweight.

For the metabolic rate assessment, we first ensured that the thyroid functions of the two groups were comparable. Both serum thyrotropin (6.67 ± 3.67 ng/ml in $AR^{L-/Y}$ mice vs. 8.22 ± 2.05 ng/ml in $AR^{X/Y}$ mice, $n$ = 6, $P > 0.05$) and 3,5,3′-triiodothyronine (0.58 ± 0.18 ng/ml in $AR^{L-/Y}$ mice versus 0.50 ± 0.11 ng/ml in $AR^{X/Y}$ mice, $n$ = 6, $P > 0.05$) were unchanged. The rectal temperatures of both groups of mice at 22 weeks of age at room temperature were similar (37.97 ± 0.46°C in $AR^{L-/Y}$ mice vs. 38.40 ± 0.43°C in $AR^{X/Y}$ mice, $P > 0.05$). We next compared the overall oxygen consumption ratio by indirect calorimetry. To minimize interference effects of the activity differences between the two groups of mice on the $Vo_2$ results, we housed the mice for calorimetry in chambers of 10 × 20 $cm^2$, which were less than one-tenth the size of the infrared frames (45 × 45 $cm^2$) used to monitor the spontaneous activities. Figure 4*A* shows representative oxygen consumption ($Vo_2$) curves of one pair of $AR^{L-/Y}$ and $AR^{X/Y}$ mice. It is apparent that besides the average level, both peaks and troughs of the curves, which represent periods of movement and resting, respectively, are generally lower in $AR^{L-/Y}$ mice. Figure 4*B* summarizes the average mean $Vo_2$; $AR^{L-/Y}$ mice consumed ~30% less oxygen than $AR^{X/Y}$ mice. These data collectively indicate that $AR^{L-/Y}$ mice had a positive energy balance, which favors the onset of obesity (25). To analyze the molecular mechanisms of the increased adiposity, we applied real-time PCR to determine the transcript levels of various genes involved in thermoregulation and lipid metabolism in WAT and BAT.

In the WAT of $AR^{L-/Y}$ mice, the expression level of the most important thermogenetic molecule, UCP-1 (26), was less than one-tenth of that in $AR^{X/Y}$ mice (Fig. 5*A*). AR is possibly a novel positive regulator of the UCP-1 gene

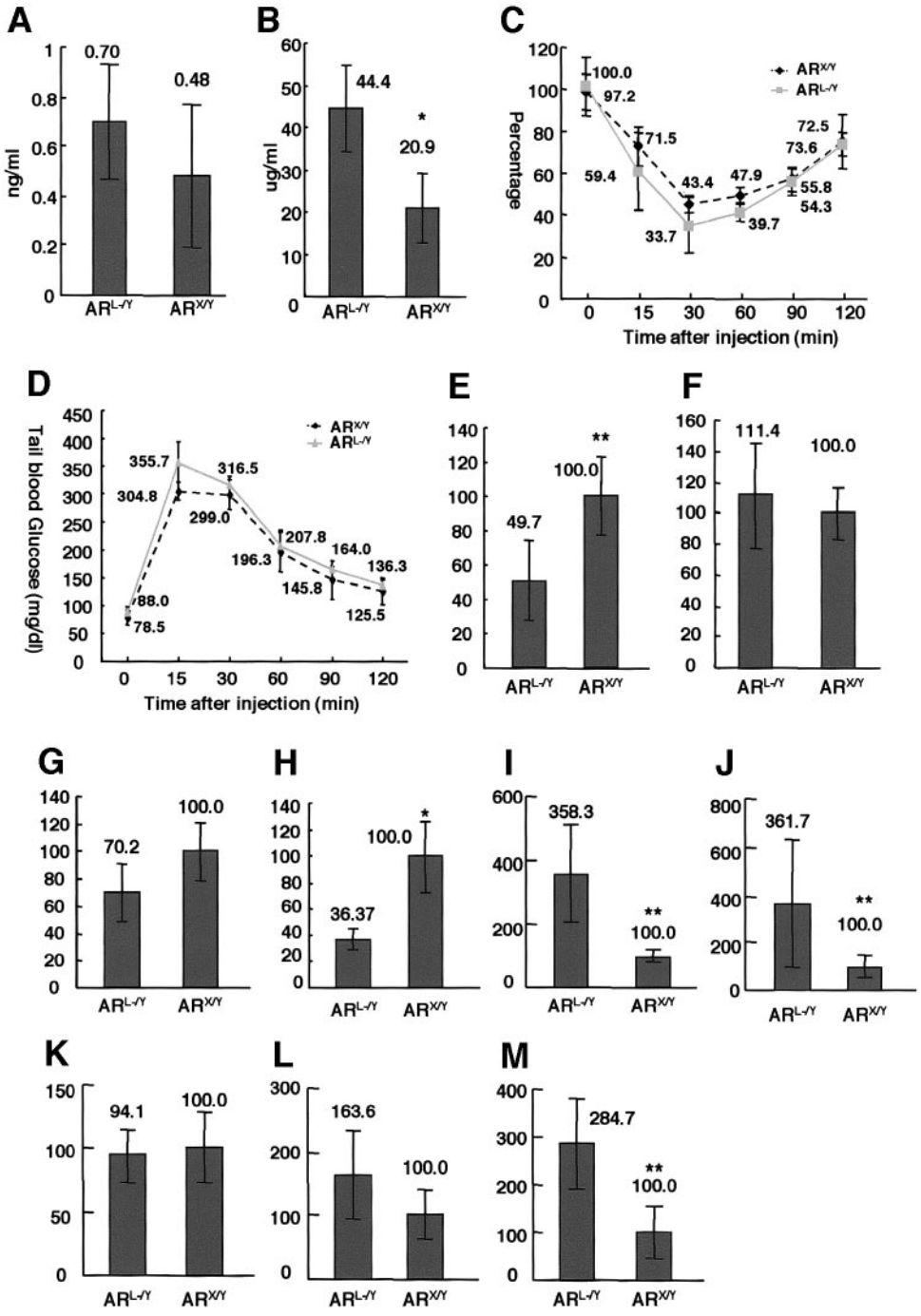


**FIG. 3. Enhanced adiponectin release from WAT and intact insulin sensitivity. *A*: Serum insulin levels in $AR^{L-/Y}$ and $AR^{X/Y}$ mice. *B*: Serum adiponectin levels in $AR^{L-/Y}$ and $AR^{X/Y}$ mice. *C*: Results of the insulin challenge test; 0.7 units regular insulin/kg body wt i.p. was injected into $AR^{L-/Y}$ and $AR^{X/Y}$ mice after overnight fasting. Tail blood glucose levels were monitored at the indicated time points. The initial glucose levels in $AR^{L-/Y}$ mice were set at 100%. *D*: Results of the intraperitoneal glucose tolerance test; 2 g D-glucose/kg body wt i.p. was injected into $AR^{L-/Y}$ and $AR^{X/Y}$ mice after overnight fasting. Tail blood glucose levels were monitored at the indicated time points. Note that there was no apparent difference in overall insulin sensitivity. *E* and *F*: Transcript levels of WAT (*E*) and BAT (*F*) adiponectin in $AR^{L-/Y}$ and $AR^{X/Y}$ mice. $AR^{X/Y}$ values were set at 100. *G*: Estimated relative total adiponectin production (RTAP) in $AR^{L-/Y}$ and $AR^{X/Y}$ mice; RTAP = %WAT × RAT, where %WAT = 100% × whole-body WAT (g)/body wt (g), and RAT is the relative adiponectin transcript copies to β-actin. $AR^{X/Y}$ values were set at 100. *H*: Transcript levels of WAT PPAR-γ in $AR^{L-/Y}$ and $AR^{X/Y}$ mice. $AR^{X/Y}$ values were set at 100. *I–M*: Transcript levels of skeletal muscle GLUT4 (*I*), hexokinase I (*J*), hexokinase II (*K*), muscle-type phosphofructokinase (*L*), and muscle-type pyruvate kinase (*M*), respectively, in both groups of mice. $AR^{X/Y}$ values were set at 100. $*P < 0.01$; $**P < 0.05$ compared with $AR^{L-/Y}$ mice ($n = 6$, except *G*, in which $n = 4$).**

because we revealed three steroid receptor response elements (TGTTCT) on a UCP-1 promoter sequence (up to −7,645 bp, GenBank accession no. U63418), and a 3.85-kb UCP-1 promoter, which contains the last consensus sequence, positively responded to AR in NIH-3T3-L1 adipocytes in a dihydrotestosterone-dependent manner (Fig. 5*B*). A decrease in UCP-1 transcript was also observed in the BAT of $AR^{L-/Y}$ mice (Fig. 5*C*), although it was less predominant than that in WAT; however, this is explained by the sevenfold higher expression of AR transcript in male WAT than BAT (Fig. 5*D*). The downregulation of UCP-1 might explain, to some extent, the lower $V_{O_2}$ in

TABLE 2
Spontaneous activity at various life stages

| Genotype | Body weight (g) | Distance (cm) | Speed composition | | | Rearing ∇ ($n$) | Rearing ∇ duration (s) |
|---|---|---|---|---|---|---|---|
| | | | % RT | % MS | % MF$^{\Delta}$ | | |
| 8 weeks | | | | | | | |
| $AR^{X/Y}$ | 23 ± 0.69 | 98,816.3 ± 10,951.0 | 60.4 | 23.9 | 15.7 | 5,026.0 ± 1067.6 | 1.12 ± 0.23 |
| $AR^{L-/Y}$ | 21 ± 1.34 | 66,394.8 ± 14,616.7* | 72.8 | 17.8 | 9.48 | 2,410.5 ± 569.5* | 1.20 ± 0.31 |
| 20 weeks | | | | | | | |
| $AR^{X/Y}$ | 31.90 ± 4.96 | 99,770.8 ± 27,281.6 | 65.8 | 20.9 | 13.3 | 7,003.2 ± 1575.7 | 1.14 ± 0.16 |
| $AR^{L-/Y}$ | 41.07 ± 3.18* | 60,608.8 ± 11,802.8* | 72.9 | 19.7 | 7.5 | 3,188.5 ± 594.3* | 1.06 ± 0.18 |
| 40 weeks | | | | | | | |
| $AR^{X/Y}$ | 35.46 ± 2.91 | 78,210.5 ± 23,996.3 | 67.4 | 21.4 | 11.2 | 3,497.7 ± 667.2 | 1.50 ± 0.24 |
| $AR^{L-/Y}$ | 56.50 ± 7.83* | 41,480.6 ± 7,164.4* | 81.8 | 13.9 | 4.2 | 1,532.8 ± 409.5* | 1.32 ± 0.43 |

*$P < 0.01$ compared with $AR^{X/Y}$ (wild-type controls), $n = 6$. ∇, rearing: mouse stands up on its hind legs. RT, resting: speed <2.00 cm/s; MS, moving slowly: speed between 2.00 and 5.00 cm/s; MF, moving fast: speed >5.00 cm/s.

$AR^{L-/Y}$ mice. In addition, another thermogenetic factor, PPAR-γ coactivator 1 (27), was also significantly decreased in both the WAT and BAT of $AR^{L-/Y}$ mice (Fig. 5*E* and *F*).

Hormone-sensitive lipase catalyzes the rate-limiting step of lipolysis in adipose tissue. The transcript level of hormone-sensitive lipase was significantly decreased in $AR^{L-/Y}$ WAT (Fig. 6*A*), whereas those for de novo lipid synthesis indicators, such as fatty acid synthase (Fig. 6*B*) and acetyl-CoA carboxylase (Fig. 6*C*) as well as the lipogenic transcriptional factor sterol regulatory element–binding protein-1c (Fig. 6*D*), were not significantly changed in both WAT and BAT (data not shown). Transcripts encoding lipoprotein lipase, the key enzyme involved in lipogenesis from circulating plasma triglyceride, were found significantly decreased in $AR^{L-/Y}$ WAT (Fig. 6*E*). The fatty acid β-oxidation markers carnitine palmitoyl transferase 1 (Fig. 6*F*) and long-chain acyl-CoA dehydrogenase (Fig. 6*G*) in $AR^{L-/Y}$ WAT showed lower trends, but they were not statistically significant. In total, decreased lipolysis rather than increased lipid synthesis might account for the increased adiposity in $AR^{L-/Y}$ mice.

## DISCUSSION

Our AR null mice have neither detectable AR transcript nor protein, thus theoretically abolishing any effect of the androgens-AR system. Mirroring the increased fat mass observed in hypogonadal men, $AR^{L-/Y}$ mice have increased body weight, which is largely attributable to expanded adiposity, as indicated by both CT-based body composition analysis and anatomy. Body weights of ARKO female mice were unchanged (10), suggesting AR's effect on adiposity is specific to males. Dysfunction of the estrogen–estrogen receptor system was reported to be associated with obesity in male subjects based on the finding from both estrogen receptor-α–knockout (19) and aromatase knockout mice (20). Although we may be unable to completely exclude a possibly mixed effect on the $AR^{L-/Y}$ obese phenotype from the estrogen–estrogen receptor system, in which the function is theoretically impaired because of the shortage of the substrate for androgen-estrogen conversion in $AR^{L-/Y}$ mice, the possibility might be minor because we noticed that serum estrogen levels in $AR^{L-/Y}$ mice at both 8 weeks (12) and 40 weeks of age remain intact compared with $AR^{X/Y}$ mice, suggesting $AR^{L-/Y}$ mice are not in short supply of estrogen. In addition, supplementation of the nonaromatizable androgen dihydrotestosterone corrected fat mass increase in castrated $AR^{X/Y}$ mice but not in $AR^{L-/Y}$ mice (10), confirming that androgen actions mediated via AR has a distinct and independent adiposity-lowering effect in male subjects. Thus, our ARKO mice represent a powerful model for studying the role of the androgen-AR system in male adiposity regulation.

The direct molecular mechanism accounting for hypertrophic adipocytes and expanded WAT of $AR^{L-/Y}$ mice might rely on the altered lipid homeostasis characterized by decreased lipolysis but not increased lipogenesis. Transcripts for hormone-sensitive lipase are strikingly decreased, whereas those for lipogenetic genes (fatty acid synthase, acetyl-CoA carboxylase, sterol regulatory element–binding protein-1c, and lipoprotein lipase) are not increased (unchanged or decreased). The results are consistent with previous suggestions that androgens are lipolytic (28,29) and are very different from those of aromatase knockout mice, in which lipogenesis was found enhanced

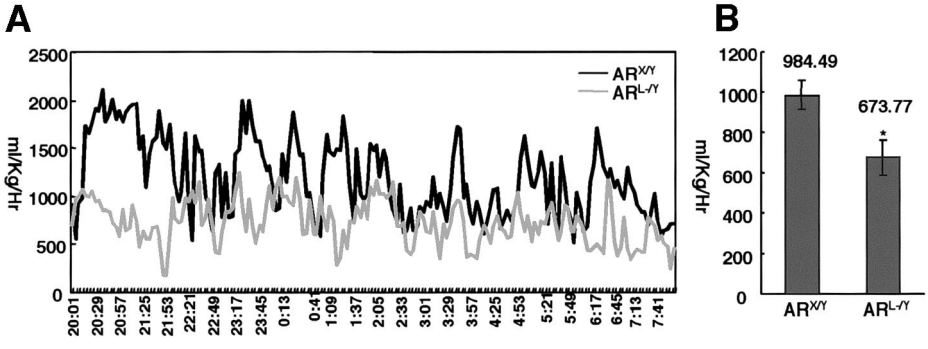


**FIG. 4. Metabolic rate assessments in $AR^{L-/Y}$ and $AR^{X/Y}$ mice. *A*: Representative oxygen consumption ($Vo_2$) tracing curves (8 P.M. to 8 A.M.). *B*: Mean average $Vo_2$ values. *$P < 0.01$ compared with $AR^{X/Y}$ mice, $n = 6$.**

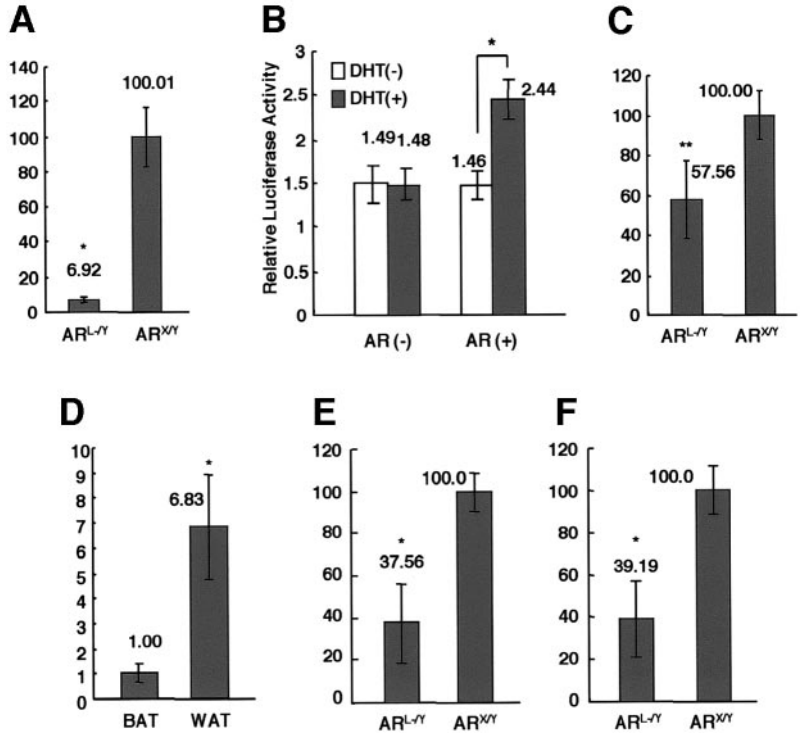


**FIG. 5. Altered expressions of UCP-1. *A*: UCP-1 transcript levels in the WAT of $AR^{L-/Y}$ and $AR^{X/Y}$ mice. $AR^{X/Y}$ values were set at 100. *B*: Dual-luciferase assay of a 3.85-kb UCP-1 promoter in NIH-3T3-L1 adipocytes. In the absence of AR, dihydrotestosterone had no effect on UCP-1 promoter; however, the promoter was activated in a dihydrotestosterone-dependent manner in the presence of AR. *C*: UCP-1 transcript levels in the BAT of $AR^{L-/Y}$ and $AR^{X/Y}$ mice. $AR^{X/Y}$ values were set at 100. *D*: Relative AR transcript levels in BAT and WAT of $AR^{X/Y}$ mice. The AR transcript levels in BAT were set at 1.00. *E* and *F*: PPAR-γ coactivator 1 transcript levels in WAT (*E*) and BAT (*F*), respectively. $AR^{X/Y}$ values were set at 100. *$P < 0.01$; **$P < 0.05$ compared with $AR^{X/Y}$ mice or BAT (*D*) ($n = 6$). DHT, dihydrotestosterone.**

(high lipoprotein lipase), but lipolysis was normal (30), suggesting estrogen is antilipogeneic.

Besides its negative role on adiposity, the androgen-AR system seems also to be negative to insulin sensitivity. Previous studies suggested androgen impairs insulin sensitivity in both humans and rodents (31,32). In our study, despite the obvious obese appearance, $AR^{L-/Y}$ mice reacted to both insulin and glucose challenges in manners that were indistinguishable from those of wild-type controls, indicating that the overall insulin sensitivity remained intact. This discordance between obesity and intact insulin-glucose homeostasis is unique to $AR^{L-/Y}$ mice, and it is very different from estrogen receptor-α knockout (19) or aromatase knockout (20) mice, which are accompanied by glucose intolerance and insulin resistance. One possible mechanism for the discordance might be hyperadiponectinemia. Adiponectin, originating from adipose tissue specifically, functions as an important insulin sensitizer (13,33) and correlates negatively with fat mass in that its plasma levels or adipose tissue mRNA levels decrease among obese subjects and recover after weight loss (34). The significant reduction of adiponectin transcripts in the WAT of obese $AR^{L-/Y}$ mice matches this conventional concept and thus suggests that downregula-

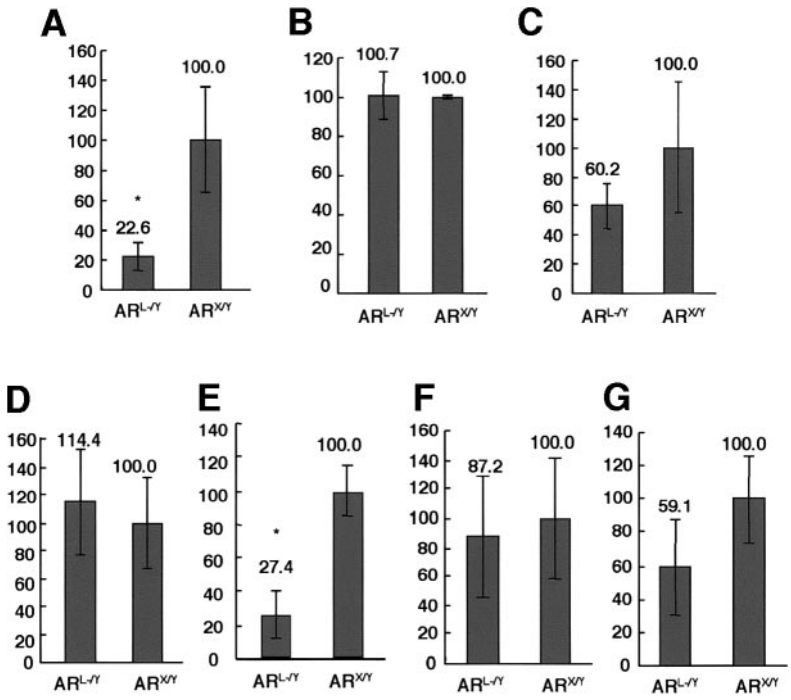


**FIG. 6. WAT transcripts levels for genes involved in lipid homeostasis. *A*: Hormone-sensitive lipase transcript levels in WAT of $AR^{L-/Y}$ and $AR^{X/Y}$ mice. *B*: Fatty acid synthase transcript levels. *C*: Acetyl-CoA carboxylase transcript levels. *D*: Sterol regulatory element–binding protein 1c transcript levels. *E*: Lipoprotein lipase transcript levels. *F*: Carnitine palmitoyl transferase 1 transcript levels. *G*: Long-chain acyl-CoA dehydrogenase transcript levels. Transcripts levels in WAT of $AR^{X/Y}$ mice were set at 100. *$P < 0.01$ compared with $AR^{X/Y}$ mice ($n = 6$).**

tion happens at the transcriptional level. However, despite the lower mRNA level in WAT tissue, the serum protein level was surprisingly elevated, even after adjustment of WAT mass, indicating that the secretion process of adiponectin protein from WAT is relatively enhanced by AR inactivation. This supports a previous suggestion that testosterone inhibits adiponectin secretion from adipocytes (35,36). Thus, the androgen-AR system is an inhibitory player in the adiponectin secretion mechanism, which is largely unclarified. The inhibitory effect may also help explain the severe insulin resistance and hypoadiponectinemia observed in diseases with androgen excess, such as polycystic ovary syndrome, in which an AR blocker was found able to improve metabolic abnormalities and dysadipocytokinemia (37). Besides hyperadiponectinemia, the low expression of PPAR-γ in $AR^{L-/Y}$ WAT may also contribute to the unexpectedly normal insulin sensitivity because an intermediate level of PPAR-γ expression in WAT is the best condition for insulin sensitivity, as suggested by the finding that heterozygous PPAR-γ–deficient mice were protected from developing insulin resistance compared with wild-type mice (23).

The molecular events behind the intact glucose homeostasis, glucose uptake, and oxidation were found enhanced in skeletal muscle by AR inactivation, mirroring the clinical picture of polycystic ovary syndrome patients, where androgen excess is related with insulin resistance (32) and impaired glucose uptake (38). However, at this moment, we're not sure whether the enhanced glucose uptake and oxidation is caused directly by androgen-AR system inactivation or is secondary to hyperadiponectinemia or low PPAR-γ expression.

Body weight and the storage of energy as triglycerides in adipose tissue are homeostatically regulated by the long-term balance between energy intake and expenditure; obesity only develops if energy intake chronically exceeds the total energy expenditure (24). Although it doesn't affect appetite, AR inactivation causes an intrinsic decrease of spontaneous physical activity in male mice as well as overall oxygen consumption ($V_{O_2}$). Thus, androgen-AR system inactivation in male mice causes a chronic positive energy balance, which favors acceleration of fat mass and obesity.

In agreement with the lower $V_{O_2}$, both the thermogenic UCP-1 and PPAR-γ coactivator 1 transcripts were decreased in the adipose tissues of $AR^{L-/Y}$ mice. UCP-1, which uncouples energy substrate oxidation from mitochondrial ATP production and hence results in a loss of potential energy as heat, is one of the most important molecules responsible for adaptive thermogenesis (26). To our knowledge, this is the first time it has been shown that AR, upon its ligand binding, directly activates UCP-1 transcription, presumably by binding to the steroid response elements on the promoter.

Although AR directly regulates factors in the peripheral tissues involved in energy homeostasis, like UCP-1, it also very likely affects the mechanism exerted by the central nervous system because AR was found densely expressed in various hypothalamic nuclei, including the ventromedial hypothalamus and dorsomedial hypothalamus and the arcuate nucleus (39). The androgen-activating 5α-reductase is also expressed in the hypothalamus (40). The physiological role of the androgen-AR system in the hypothalamus is largely unknown. It is highly possible that the receptor may be involved in regulating the leptin-regulated melanocortin circuit because AR activation in the hypothalamus increases the inhibitory neuropeptide somatostatin (41,42), which may in turn inhibit the anorexigenic melanocyte-stimulating hormone or cocaine- and amphetamine-regulated transcript. The altered energy balance in $AR^{L-/Y}$ characterized by lower $V_{O_2}$ and lower physical activity warrants further study of the intra–central nervous system role of AR, which is now ongoing.

In summary, the androgen-AR system is correlated with male adiposity, and inactivation of the system causes late-onset obesity in male mice because of altered energy balance, since the $AR^{L-/Y}$ mice were euphagic but less physically dynamic and less oxygen-consuming compared with $AR^{X/Y}$ mice. The mechanism of decreased energy expenditure might reside in both the central nervous system and peripheral tissues. Besides its negative role in adiposity, the androgen-AR system also plays a negative role in insulin sensitivity, at least in part through inhibiting the release of adiponectin from adipose tissue.

## ACKNOWLEDGMENTS

This work was supported in part by a grant for the 21st Century COE Program from the Japanese Ministry of Education, Culture, Sports, Science, and Technology.

## REFERENCES

1. Gustafson DR, Wen MJ, Koppanati BM: Androgen receptor gene repeats and indices of obesity in older adults. *Int J Obes Relat Metab Disord* 27:75–81, 2003
2. Jorgensen JO, Vahl N, Hansen TB, Fisker S, Hagen C, Christiansen JS: Influence of growth hormone and androgens on body composition in adults. *Horm Res* 45:94–98, 1996
3. Vermeulen A: Andropause. *Maturitas* 34:5–15, 2000
4. Kyle UG, Genton L, Hans D, Karesgard L, Slosman DO, Pichard C: Age-related differences in fat-free mass, skeletal muscle, body cell mass and fat mass between 19 and 94 years. *Eur J Clin Nutr* 55:663–672, 2001
5. Matsumoto AM: Andropause: clinical implications of the decline in serum testosterone levels with aging in men. *J Gerontol A Biol Sci Med Sci* 57:M76–M99, 2002
6. Katznelson L, Rosenthal DI, Rosol MS, Anderson EJ, Hayden DL, Schoenfeld DA, Klibanski A: Using quantitative CT to assess adipose distribution in adult men with acquired hypogonadism. *Am J Roentgenol* 170:423–427, 1998
7. Rolf C, von Eckardstein S, Koken U, Nieschlag E: Testosterone substitution of hypogonadal men prevents the age-dependent increases in body mass index, body fat and leptin seen in healthy ageing men: results of a cross-sectional study. *Eur J Endocr* 146:505–511, 2002
8. Wang C, Swedloff RS, Iranmanesh A, Dobs A, Snyder PJ, Cunningham G, Matsumoto AM, Weber T, Berman N: Transdermal testosterone gel improves sexual function, mood, muscle strength, and body composition parameters in hypogonadal men. *J Clin Endocrinol Metab* 85:2839–2853, 2000
9. Mauras N, Hayes V, Welch S, Rini A, Helgeson K, Dokler M, Veldhuis JD, Urban RJ: Testosterone deficiency in young men: marked alterations in whole body protein kinetics, strength, and adiposity. *J Clin Endocrinol Metab* 83:1886–1992, 1998
10. Sato T, Matsumoto T, Yamada T, Watanabe T, Kawano H, Kato S: Late onset of obesity in male androgen receptor-deficient (AR KO) mice. *Biochem Biophys Res Commun* 300:167–171, 2003
11. Sato T, Matsumoto T, Kawano H, Watanabe T, Uematsu Y, Sekine K, Fukuda T, Aihara K, Krust A, Yamada T, Kato S: Brain masculinization requires androgen receptor function. *Proc Natl Acad Sci U S A* 101:1673–1678, 2004
12. Kawano H, Sato T, Yamada T, Matsumoto T, Sekine K, Watanabe T, Nakamura T, Fukuda T, Yoshimura K, Yoshizawa T, Kato S: Suppressive function of androgen receptor in bone resorption. *Proc Natl Acad Sci U S A* 100:9416–9421, 2003

13. Maeda N, Shimomura I, Kishida K, Nishizawa H, Matsuda M, Nagaretani H, Furuyama N, Kondo H, Takahashi M, Arita Y, Komuro R, Ouchi N, Kihara S, Tochino Y, Okutomi K, Horie M, Takeda S, Aoyama T, Funahashi T, Matsuzawa Y: Diet-induced insulin resistance in mice lacking adiponectin/ACRP30. *Nat Med* 8:731–737, 2002
14. Fan W, Yanase T, Morinaga H, Mu YM, Nomura M, Okabe T, Goto K, Harada N, Nawata H: Activation of peroxisome proliferator-activated receptor-gamma and retinoid X receptor inhibits aromatase transcription via nuclear factor-kappaB. *Endocrinology* 146:85–92, 2005
15. Fan W, Yanase T, Wu Y, Kawate H, Saitoh M, Oba K, Nomura M, Okabe T, Goto K, Yanagisawa J, Kato S, Takayanagi R, Nawata H: Protein kinase A potentiates adrenal 4 binding protein/steroidogenic factor 1 transactivation by reintegrating the subcellular dynamic interactions of the nuclear receptor with its cofactors, general control nonderepressed-5/transformation/transcription domain-associated protein, and suppressor, dosage-sensitive sex reversal-1: a laser confocal imaging study in living KGN cells. *Mol Endocrinol* 18:127–141, 2004
16. Broulik PD, Schreiber V: Effect of alloxan diabetes on kidney growth in intact and castrated mice. *Acta Endocrinol* 99:109–111, 1982
17. Avdalovic N, Bates M: The influence of testosterone on the synthesis and degradation rate of various RNA species in the mouse kidney. *Biochim Biophys Acta* 407:299–307, 1975
18. Bachman ES, Dhillon H, Zhang CY, Cinti S, Bianco AC, Kobilka BK, Lowell BB: betaAR signaling required for diet-induced thermogenesis and obesity resistance. *Science* 297:843–845, 2002
19. Heine PA, Taylor JA, Iwamoto GA, Lubahn DB, Cooke PS: Increased adipose tissue in male and female estrogen receptor-alpha knockout mice. *Proc Natl Acad Sci U S A* 97:12729–12734, 2000
20. Jones ME, Thorburn AW, Britt KL, Hewitt KN, Wreford NG, Proietto J, Oz OK, Leury BJ, Robertson KM, Yao S, Simpson ER: Aromatase-deficient (ArKO) mice have a phenotype of increased adiposity. *Proc Natl Acad Sci U S A* 97:12735–12740, 2000
21. Simpson ER, Davis SR: Another role highlighted for estrogens in the male: sexual behavior. *Proc Natl Acad Sci U S A* 97:14038–14040, 2000
22. Combs TP, Berg AH, Philipp SB, Scherer E, Rossetti L: Endogenous glucose production is inhibited by the adipose-derived protein Acrp30. *J Clin Invest* 108:1875–1881, 2001
23. Kubota N, Terauchi Y, Miki H, Tamemoto H, Yamauchi T, Komeda K, Satoh S, Nakano R, Ishii C, Sugiyama T, Eto K, Tsubamoto Y, Okuno A, Murakami K, Sekihara H, Hasegawa G, Naito M, Toyoshima Y, Tanaka S, Shiota K, Kitamura T, Fujita T, Ezaki O, Aizawa S, Kadowaki T: PPAR gamma mediates high-fat diet-induced adipocyte hypertrophy and insulin resistance. *Mol Cell* 4:597–609, 1999
24. Spiegelman BM, Flier JS: Obesity and the regulation of energy balance. *Cell* 104:531–543, 2001
25. Lowell BB, Spiegelman BM: Towards a molecular understanding of adaptive thermogenesis. *Nature* 404:652–660, 2000
26. Argyropoulos G, Harper ME: Uncoupling proteins and thermoregulation. *J Appl Physiol* 92:2187–2198, 2002
27. Puigserver P, Spiegelman BM: Peroxisome proliferator-activated receptor-gamma coactivator 1 alpha (PGC-1 alpha): transcriptional coactivator and metabolic regulator. *Endocr Rev* 24:78–90, 2003
28. Xu X, De Pergola G, Bjorntorp P: The effects of androgens on the regulation of lipolysis in adipose precursor cells. *Endocrinology* 126:1229–1234, 1990
29. Sih R, Morley JE, Kaiser FE, Perry III HM, Patrick P, Ross C: Testosterone replacement in older hypogonadal men: a 12-month randomized controlled trial. *J Clin Endocrinol Metab* 82:1661–1667, 1997
30. Misso ML, Murata Y, Boon WC, Jones ME, Britt KL, Simpson ER: Cellular and molecular characterization of the adipose phenotype of the aromatase-deficient mouse. *Endocrinology* 144:1474–1480, 2003
31. Shoupe D, Lobo RA: The influence of androgens on insulin resistance. *Fertil Steril* 41:385–388, 1984
32. Toprak S, Yonem A, Cakir B, Guler S, Azal O, Ozata M, Corakci A: Insulin resistance in nonobese patients with polycystic ovary syndrome. *Horm Res* 55:65–70, 2001
33. Yamauchi T, Kamon J, Waki H, Imai Y, Shimozawa N, Hioki K, Uchida S, Ito Y, Takakuwa K, Matsui J: Globular adiponectin protected ob/ob mice from diabetes and ApoE-deficient mice from atherosclerosis. *J Biol Chem* 278:2461–2468, 2003
34. Pittas AG, Joseph NA, Greenberg AS: Adipocytokines and insulin resistance. *J Clin Endocrinol Metab* 89:447–452, 2004
35. Nishizawa H, Shimomura I, Kishida K, Maeda N, Kuriyama H, Nagaretani H, Matsuda M, Kondo H, Furuyama N, Kihara S, Nakamura T, Tochino Y, Funahashi T, Matsuzawa Y: Androgens decrease plasma adiponectin, an insulin-sensitizing adipocyte-derived protein. *Diabetes* 51:2734–2741, 2002
36. Lanfranco F, Zitzmann M, Simoni M, Nieschlag E: Serum adiponectin levels in hypogonadal males: influence of testosterone replacement therapy. *Clin Endocrinol* (*Oxf*) 60:500–507, 2004
37. Ibanez L, Valls C, Cabre S, De Zegher F: Flutamide-metformin plus ethinylestradiol-drospirenone for lipolysis and antiatherogenesis in young women with ovarian hyperandrogenism: the key role of early, low-dose flutamide. *J Clin Endocrinol Metab* 89:4716–4720, 2004
38. Holte J: Polycystic ovary syndrome and insulin resistance: thrifty genes struggling with over-feeding and sedentary life style? *J Endocrinol Invest* 21:589–601, 1998
39. Herbison AE: Neurochemical identity of neurones expressing oestrogen and androgen receptors in sheep hypothalamus. *J Reprod Fertil Suppl* 49:271–283, 1995
40. Poletti A, Martini L: Androgen-activating enzymes in the central nervous system. *J Steroid Biochem Mol Biol* 69:117–122, 1999
41. Zeitler P, Vician L, Chowen-Breed JA, Argente J, Tannenbaum GS, Clifton DK, Steiner RA: Regulation of somatostatin and growth hormone-releasing hormone gene expression in the rat brain. *Metabolism* 39:46–49, 1990
42. Hasegawa O, Sugihara H, Minami S, Wakabayashi I: Masculinization of growth hormone (GH) secretory pattern by dihydrotestosterone is associated with augmentation of hypothalamic somatostatin and GH-releasing hormone mRNA levels in ovariectomized adult rats. *Peptides* 13:475–481, 1992